Title

Adenylyl cyclase 9 is auto-stimulated by its isoform-specific carboxyl terminal domain and equipped with paradigm-switching mechanisms.

Zhihao Chen* and Ferenc A. Antoni

Centre for Discovery Brain Sciences, Deanery of Biomedical Sciences, University of Edinburgh, Edinburgh, Scotland, U.K.

Corresponding author:

Ferenc A. Antoni

Centre for Discovery Brain Sciences, Deanery of Biomedical Sciences, University of Edinburgh, Edinburgh, Scotland, U.K.

mailto:ferenc.antoni@ed.ac.uk

* Work done in lieu of an MScR degree in Biomedical Sciences.

Abstract

Transmembrane adenylyl cyclase 9 (AC9) is unusual in not being regulated by heterotrimeric G proteins. The key to resistance to stimulation by Gs-coupled receptors (GsR) is auto-inhibition by the COOH-terminal domain (C2b). Surprisingly, we found C2b to be essential in sustaining the high basal output of cyclic AMP by AC9, which is regulated by intracellular free Ca^{2+} and calcineurin. A human mutation (E326D) in the parallel coiled-coil formed by the signalling helices of AC9 dramatically increased basal activity, which was dependent on the C2b domain. Intriguingly, the same mutation enabled stimulation of AC9 by GsRs. In summary, the C2b domain of AC9 sustains its basal activity (auto-stimulation) and quenches activation by GsR (auto-inhibition). Thus AC9 is tailored to support constitutive phosphorylation by protein kinase A. A switch from this paradigm to stimulation by GsRs may be occasioned by conformation changes at the coiled-coil or removal of the C2b domain.

Transmembrane adenylyl cyclases produce the ubiquitous signalling molecule adenosine-3':5'-monophosphate (cAMP). Nine genes encode these enzymes in mammals and each paralogue has unique regulatory properties [1]. Adenylyl cyclase 9 (AC9) is widely distributed in the body and has been implicated in a number of physiological processes, including cardiac function, body fat mass and body weight, as well as cancer pathologies reviewed in ref. [2]. Partial high-resolution maps of the structure of AC9 obtained by cryo-electronmicroscopy (cryoEM) have been recently published [3,4]. In brief, the 1353-residue single polypeptide chain of AC9 is arranged into a tripartite structure. This consists of a large trans-membrane array that is connected to the catalytic domain in the cytoplasm by two alpha helices (Fig 1). The helices form a short parallel coiled-coil in close proximity to the catalytic core (Fig 1). Sequence alignments of human adenylyl cyclases indicate that the coiled-coil of the "signalling helices" [5,6] is a generic feature of these proteins (Fig 2A). Coiled-coils are

important regulatory modules in several proteins [7] including soluble guanylyl cyclases where the binding of nitric oxide is transmitted to the catalytic domains through conformational changes of the signalling helix [8]. As full-length AC9 is largely insensitive to heterotrimec G proteins [4,9,10] the coiled-coil as a potential regulator enzymatic activity is of particular interest. Here, we analysed the effects of two single amino-acid mutations, L323S and E326D on cAMP production by human AC9. Both of these mutations are at the interface of the coiled-coil, E326D was found in a human thyroid adenoma [11] while a mutation homologous to L323S produced constitutive activation of *Dyctiostelium discoideum* adenylyl cyclase [12]. We report that the coiled-coil has a major influence on enzymatic activity exerted in conjunction with the isoform-specific carboxyl terminal C2b domain of AC9.

Results

Selective effects of coiled-coil mutations

Mutation L394S, which is in the homologous position for L323 in human AC9, caused constitutive activation of *Dyctiostelium discoideum* adenylyl cyclase [12]. However, there were no discernible changes of basal or isoproterenol-induced cAMP production by L323S_AC9 when compared to the wild-type enzyme (not shown). Notably, while eight of nine isoforms of mammalian transmembrane adenylyl cyclase have leucine at the position homologous to L323, AC5 has a serine (Fig 2C). Thus, the mammalian enzymes may tolerate this mutation.

In sharp contrast, mutation E326D caused a 10-fold increase of basal cAMP production as well as an enhancement of the cAMP response to isoproterenol (Fig 3). Notably, as reported previously in a different *in transfecto* assay [10], no consistent isoproterenol-induced cAMP response attributable to wild-type AC9 could be discerned. Previously, the basal production of cAMP by AC9 could be only unmasked by inhibitors of cyclic nucleotide hydrolysing phosphodiesterases in HEK293 cells stably over-expressing AC9 [13]. In contrast, the high levels of protein

expression in HEK293FT cells allowed us to clearly demonstrate that basal cAMP levels were increased at least ten-fold upon transient expression of AC9 (Fig3 and Fig4A insert).

Probing the role of the C2b domain

Previous work has shown that the isoform-specific C2b domain of AC9 quenches the activation of AC9 by Gs-coupled receptors [4,10]. Surprisingly, removal of the C2b domain from E326D_AC9 as well as wild-type AC9 reduced basal cAMP levels by 80-90% (Fig 4A and B). With respect stimulation by GsR, the amplitude of the agonist-induced cAMP response of AC9C2a was dramatically enhanced when compared with full-length AC9 (Fig 3A). However, this was not the case for E326D_AC9C2a: the peak levels of cAMP and the time-course of the isoproterenol response were not significantly different from those of full-length E326D_AC9 at any concentration of agonist tested indicating that the efficacy of auto-inhibition through AIM was drastically reduced by the E326D mutation. Closely similar results were obtained with prostaglandin E1 as the agonist (data not shown). The lack of an enhancement of the response to isoproterenol in E326D_AC9C2a is unlikely to be due to the saturation of Glosensor22F as it was apparent with all agonist-induced responses that evoked light-emission well below those elicited by the forskolin/rolipram stimulus. As a quality control for glosensor22F expression was run in each well and the levels of expression of the respective AC9 proteins show variations not greater that two-fold [10], it is justified to conclude that the dramatic differences of cellular cAMP levels observed in our experiments largely reflect the respective rates of cAMP production.

Discussion

The first important novel finding of this study is that the C2b domain sustains the high basal activity of AC9. We also confirmed and extended previous results [4,10] that the C2b quenches Gsα induced activation. The second significant new result is that the

coiled-coil of the AC9 transduction helices has a major influence on catalytic activity and can differentially modify the influence of the C2b domain.

The isoform-specific C2b domain is essential for sustaining unstimulated or “basal” cAMP production by AC9. Thus AC9 is an auto-stimulated enzyme in this respect. The role of C2b was readily apparent in wild-type as well as E326D mutant AC9. Importantly, basal cAMP production by AC9 is regulated by an intracellular pathway involving Ca^{2+} and calcineurin [13-15]. It is also known that AC9 is insensitive to the trimeric G proteins Gi and Go, as well as $G\beta\gamma$ subunits [9,16]. Moreover, auto-inhibition by C2b quenches the activation by $Gs\alpha$ [4,10]. Thus full-length AC9 largely filters out input from G proteins activated by cell-surface receptors whilst having auto-stimulated high basal activity regulated by intracellular free Ca^{2+}. As such, it is ideally suited to populate cAMP nanodomains that require constitutive activity of cAMP effector proteins [17], above all, protein kinase A. Amongst others, the maintenance of releasable pools of secretory vesicles [18], the activity of ion-channels [19,20] and vesicle trafficking in the trans-Golgi network require such characteristics [21]. Indeed, AC9 has been specifically implicated in the latter process [22].

In another setting, expression of high levels of auto-stimulated AC9 may promote growth or regeneration or cell death depending on the cellular environment [23]. In this context, the regulation of the expression of AC9 becomes an important issue in cancer biology [24-28]. With respect to somatic mutations, the introduction of aspartate instead of glutamate at the coiled-coil interface (E326D) in all probability changes the conformation of the coil [29,30]. In the case of E326D_AC9 this led to a large, close to ten-fold increase in basal enzymatic activity. In parallel, the cAMP response to receptor activation appeared, indicating a release from the potent autoinhibitory effect exerted by the C2b domain [4,10]. The presence of such an adenylyl cyclase in

thyroid epithelial cells [11] is likely to lead to hypertrophy and hyperplasia. In the context of a second oncogenic mutation, it can support adenomatous hyperproliferation [11] or epithelial mesenchymal transition producing malignant tumour growth [25].

In a yet further aspect, the sensitivity of AC9 enzymatic activity to the conformation of the coiled-coil coupled with the exclusion of input from G proteins suggest that AC9 could be poised to respond selectively to conformational changes at the interface of transmembrane coils 6 and 12 [4] (Fig 1). This may be transmitted to the coiled-coil and further modulated by a phosphorylation cluster located between the coiled-coil and the catalytic core [2,6]. Overall, this scenario is similar to the activation of soluble guanylyl cyclase by NO [8]. However, in the case of AC9 the transmembrane domains could function as cell-surface receptors and/or sensors of the lipid composition of the plasma membrane [3,4,31,32]. With respect to protein phosphorylation, functionally relevant activation of AC9 by protein kinase cascades independently of Gs has been reported in neutrophil granulocytes [33]. Last but not least, AC9 may be recruited into the GsR regulatory circuit by proteolytic cleavage of the COOH-terminal C2b domain, which markedly lowers basal activity and enables the response to Gsα. This appears to be prominent in heart tissue and AtT20 pituitary tumour cells [10]. Figure 5 shows the three modes of operation of AC9 discussed above. In principle, all three may occur simultaneously in the same cell.

In summary, AC9 features auto-stimulation of basal activity as well as auto-inhibition of Gsα activation by its isoform-specific C2b domain. The full-length enzyme is insensitive to regulation by heterotrimeric G proteins. These facets of autoregulation are differentially modulated by the coiled-coil of the signalling helices. As AC9 is

widely distributed in the body, these features of intracellular cAMP signalling are bound to be relevant in several organ systems.

Acknowledgments

We would like thank Miss Heather McClafferty for help with cell lines and various reagents, Dr Paul LeTissier for access to a luminometer, Prof Mike Shipston, Dr Paul Skehel and Dr Tamás Balla for helpful discussions, Dr Mandy Jackson and Dr Paul Skehel for access to laboratory facilities and reagents.

References

1. Ostrom, K.F. et al. Physiological roles of mammalian transmembrane adenylyl cyclase isoforms. *Physiol Rev* **102**, 815-857 (2022).
2. Antoni, F.A. The chilling of adenylyl cyclase 9 and its translational potential. *Cell Signal* **70**, 109589 (2020).
3. Qi, C. et al. Structural basis of adenylyl cyclase 9 activation. *Nat Commun* **13**, 1045 (2022).
4. Qi, C., Sorrentino, S., Medalia, O. & Korkhov, V.M. The structure of a membrane adenylyl cyclase bound to an activated stimulatory G protein. *Science* **364**, 389-394 (2019).
5. Bassler, J., Schultz, J.E. & Lupas, A.N. Adenylate cyclases: Receivers, transducers, and generators of signals. *Cell Signal* **46**, 135-144 (2018).
6. Anantharaman, V., Balaji, S. & Aravind, L. The signaling helix: a common functional theme in diverse signaling proteins. *Biol Direct* **1**, 25 (2006).
7. Lupas, A.N. & Bassler, J. Coiled Coils - A Model System for the 21st Century. *Trends Biochem Sci* **42**, 130-140 (2017).
8. Horst, B.G. et al. Allosteric activation of the nitric oxide receptor soluble guanylate cyclase mapped by cryo-electron microscopy. *Elife* **8**(2019).
9. Baldwin, T.A., Li, Y., Brand, C.S., Watts, V.J. & Dessauer, C.W. Insights into the regulatory properties of human adenylyl cyclase type 9. *Mol Pharmacol* **95**, 349-360 (2019).
10. Pálvölgyi, A. et al. Auto-inhibition of adenylyl cyclase 9 (AC9) by an isoform-specific motif in the carboxyl-terminal region. *Cell Signal* **51**, 266-275 (2018).
11. Calebiro, D. et al. Recurrent EZH1 mutations are a second hit in autonomous thyroid adenomas. *J Clin Invest* **126**, 3383-8 (2016).
12. Parent, C.A. & Devreotes, P.N. Constitutively active adenylyl cyclase mutant requires neither G proteins nor cytosolic regulators. *J Biol Chem* **271**, 18333-6 (1996).
13. Antoni, F.A. et al. Ca2+/calcineurin-inhibited adenylyl cyclase highly abundant in forebrain regions important for learning and memory. *J of Neurosci* **18**, 9650-9661 (1998).
14. Antoni, F.A. et al. Calcineurin feedback inhibition of agonist-evoked cAMP formation. *J Biol Chem* **270**, 28055-28061 (1995).
15. Paterson, J.M., Smith, S.M., Harmar, A.J. & Antoni, F.A. Control of a novel adenylyl cyclase by calcineurin. *Biochem Biophys Res Com* **214**, 1000-1008 (1995).

16. Premont, R.T. et al. Identification and characterization of a widely expressed form of adenylyl cyclase. *J Biol Chem* **271**, 13900-7 (1996).
17. Marsden, A.N. & Dessauer, C.W. Nanometric targeting of type 9 adenylyl cyclase in heart. *Biochem Soc Trans* **47**, 1749-1756 (2019).
18. Nagy, G. et al. Regulation of releasable vesicle pool sizes by protein kinase A-dependent phosphorylation of SNAP-25. *Neuron* **41**, 417-29 (2004).
19. Antos, C.L. et al. Dilated cardiomyopathy and sudden death resulting from constitutive activation of protein kinase a. *Circ Res* **89**, 997-1004 (2001).
20. Baldwin, T.A. et al. Popeye domain-containing protein 1 scaffolds a complex of adenylyl cyclase 9 and the two-pore-domain potassium channel TERK-1 in heart. (2021).
21. Muniz, M., Martin, M.E., Hidalgo, J. & Velasco, A. Protein kinase A activity is required for the budding of constitutive transport vesicles from the trans-Golgi network. *Proc Natl Acad Sci U S A* **94**, 14461-6 (1997).
22. Cancino, J. et al. Control systems of membrane transport at the interface between the endoplasmic reticulum and the Golgi. *Dev Cell* **30**, 280-94 (2014).
23. Insel, P.A., Zhang, L., Murray, F., Yokouchi, H. & Zambon, A.C. Cyclic AMP is both a pro-apoptotic and anti-apoptotic second messenger. *Acta Physiol (Oxf)* **204**, 277-87 (2012).
24. Johannessen, C.M. et al. A melanocyte lineage program confers resistance to MAP kinase pathway inhibition. *Nature* **504**, 138-42 (2013).
25. Tan, X. et al. The epithelial-to-mesenchymal transition activator ZEB1 initiates a prometastatic competing endogenous RNA network. *J Clin Invest* **128**, 1267-1282 (2018).
26. Yang, L. et al. miR-181b promotes cell proliferation and reduces apoptosis by repressing the expression of adenylyl cyclase 9 (AC9) in cervical cancer cells. *FEBS Lett* **588**, 124-30 (2014).
27. Yi, H. et al. Elevated adenylyl cyclase 9 expression is a potential prognostic biomarker for patients with colon cancer. *Med Sci Monit* **24**, 19-25 (2018).
28. Milan, T. et al. Epigenetic changes in human model KMT2A leukemias highlight early events during leukemogenesis. *Haematologica* **107**, 86-99 (2022).
29. Straussman, R., Ben-Ya'acov, A., Woolfson, D.N. & Ravid, S. Kinking the coiled coil--negatively charged residues at the coiled-coil interface. *J Mol Biol* **366**, 1232-42 (2007).
30. Jonson, P.H. & Petersen, S.B. A critical view on conservative mutations. *Protein Eng* **14**, 397-402 (2001).
31. Finkbeiner, M., Grischin, J., Seth, A. & Schultz, J.E. In search of a function for the membrane anchors of class IIIa adenylate cyclases. *Int J Med Microbiol* **309**, 245-251 (2019).
32. Seth, A., Finkbeiner, M., Grischin, J. & Schultz, J.E. Gsalpha stimulation of mammalian adenylate cyclases regulated by their hexahelical membrane anchors. *Cell Signal* **68**, 109538 (2020).
33. Liu, L., Das, S., Losert, W. & Parent, C.A. mTORC2 regulates neutrophil chemotaxis in a cAMP- and RhoA-dependent fashion. *Dev Cell* **19**, 845-57 (2010).
34. Xia, Y., Chu, W., Qi, Q. & Xun, L. New insights into the QuikChange process guide the use of Phusion DNA polymerase for site-directed mutagenesis. *Nucl Acids Res* **43**, e12 (2015).
35. Binkowski, B.F. et al. A luminescent biosensor with increased dynamic range for intracellular cAMP. *ACS Chem Biol* **6**, 1193-7 (2011).

Figures

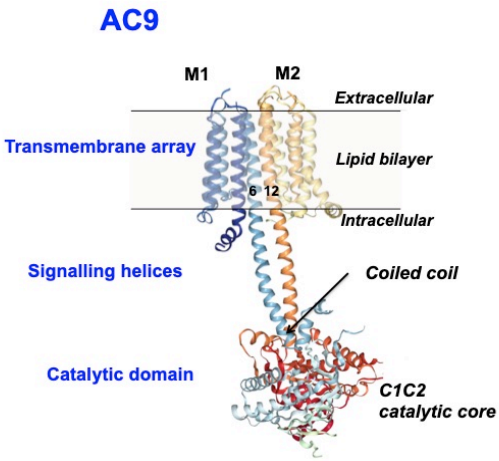

Figure 1 The tripartite structure of AC9 derived from cryoEM studies by Qi and co-workers [3,4]. Note that the enzyme consists of a 1353-residue single polypeptide and that some parts of the protein have not been resolved in the cryoEM studies [2]. Transmembrane helices 6 and 12 are interfaced in the lipid bilayer and continue into the cytoplasm as the signalling helices that form a short, parallel coiled-coil just above the catalytic domain.

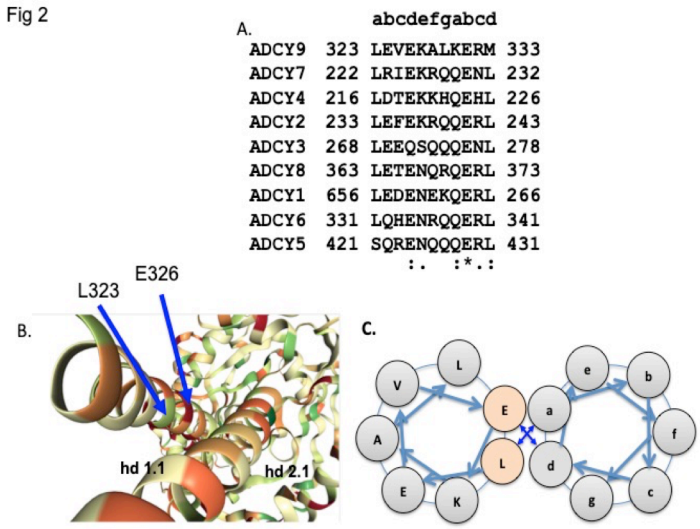

Figure 2. Schematic representation of the mutations studied in the coiled-coil of AC9. (A) Alignment of the hd1.1 segment (4,5) of human adenylyl cyclase paralogues. The small lettering in the top row indicates the positions in the coiled-

coiled heptad of bovine AC9 (B) Both L323 and E326 are at the interface of the coiled-coil, at positions *a* and *d,* respectively of the heptad repeat as schematically shown in (C).

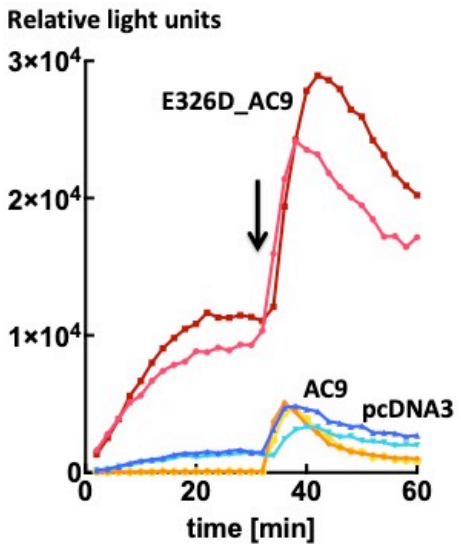

Figure 3. Point-mutation E326D markedly enhances cellular levels of cAMP. Intracellular levels of cAMP reported by Glosensor22F firefly luciferase bioluminescence in HEK293FT cells transiently transfected with AC9, E326D_AC9 or the skeleton vector pcDNA3. Isoproterenol (10 nM) was applied as indicated by the arrow. Single data-points recorded from individual wells of a 96-well microtiter plate are shown. Representative of at least six experiments from at least three different batches of transfected cells yielding closely similar results.

Fig 4

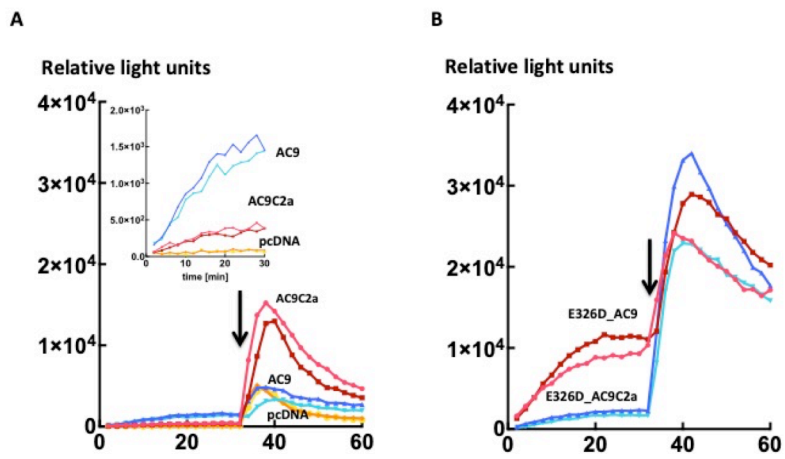

Figure 4. Effects of removing the isoform-specific C2b domain on intracellular levels of cAMP reported by Glosensor22F firefly luciferase bioluminescence from (A) HEK293FT cells transiently transfected with AC9, AC9C2a or pcDNA3. The insert shows the basal cAMP levels from the same wells. The traces of AC9 and pcDNA3 are the ones already shown in Fig. 3 (B) HEK293FT cells transiently transfected with E326D_AC9 or E326D_AC9C2a. The traces of E326D_AC9 are the ones already shown in Fig. 3. Isoproterenol (10 nM) was applied as indicated by the arrow. Single data points from individual wells of a 96-well microtiter plate. Representative of six experiments from at least three different batches of transfected cells yielding closely similar results.

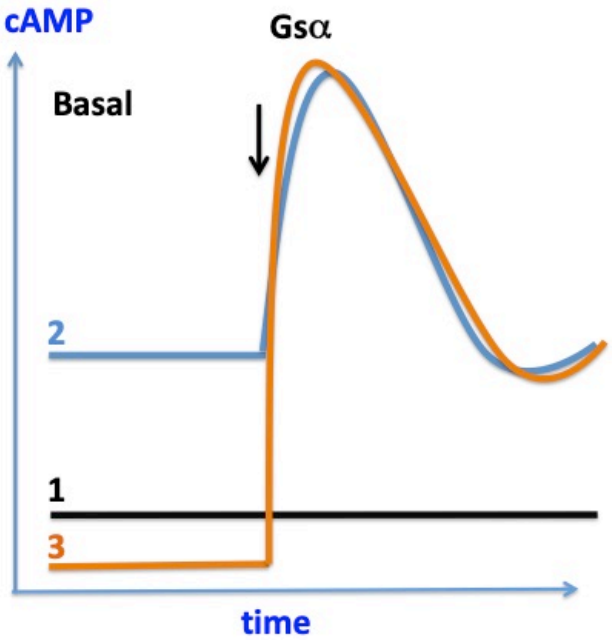

Fig 5: Three modes of operation of AC9 as indicated by this study and previous work. Mode 1: High basal activity supported by the C2b domain and quenching of activation "occluded state" in the presence of activated Gsα, as shown in previous work. Importantly, the production of cAMP by AC9 is inhibited by intracellular free Ca2+ through calcineurin. Mode 2: Conformation change at the coiled coil enhances basal activity dependent on C2b and relieves the quenching of the activation by Gsα. Mode 3 : Removal of the C2b domain markedly reduces basal activity and enables stimulation by Gsα, i.e. AC9 now resembles a conventional adenylyl cyclase stimulated by Gsα.

Online Methods

Human AC9 tagged with HA at the N-terminus and FLAG at the C-terminus in pcDNA3.1 (AC9) was a gift of Dr. Adrienn Pálvölgyi (Egis PLC, Budapest, Hungary). This construct was used for site-directed mutagenesis with Phusion polymerase (NEB, Ipswich, MA.,U.S.A.) following previously published protocols [34]. Two mutations were produced - L323S and E326D. Both amino acid residues are part of the

interface of the coiled-coil of AC9 (Fig 2B and C). Subsequently, the C2b domain was removed from AC9 and E326D_AC9 [10] to encode AC9_C2a and E326D_AC9C2a, respectively. The sites of the mutations as well as the N- and C-terminal coding sequences were verified by Big Dye sequencing. Fast-growing human embryonic kidney 293T cells (HEK293FT) were maintained in DMEM 10% FBS (v/v) and passaged at 5-7 day intervals with TrypleExpress (Invitrogen) to detach the cells. About 2 million cells in 1.6 ml of growth medium were mixed with 4 µg of AC9 cDNA or 2µg of pcDNA3 plus 2 µg of GlosensorF22 pre-complexed with Lipofectamine 2000 in 400 µl OPTIMEM. After 48h, the cells were plated in poly-l-lysine coated, 96well white tissue culture plates (Greiner) at 10^5 cells per well and incubated as above for 24 h. The luminescence signal was recorded in a BMG Lumistar Omega plate-reader after cells had been depleted of serum for 1h and incubated in Hank's balanced salt solution containing 1 mM MgSO4, 1.5 mM $CaCl_2$, 10 mM HEPES pH7.4 and 1 mM beetle luciferin (Promega) at 32°C for 60 min. Luminescence from each well was recorded at 2 min intervals for up to 3 h. Drug treatments were added from a 12-channel hand-held pipette. Due to the inherent variability of transient transfections each well received a mixture of 5 µM forskolin (LC labs, Woburn, MA, U.S.A.) and 100 µM rolipram (Insight Biotech, Wembley, U.K.) at the end of the recording as a quality control stimulus. This standardization was possible because AC9 is minimally stimulated by forskolin even when stimulated by Gsα [3,4,9]. As the glosensor response at high levels of cAMP becomes non-linear and eventually saturates [35], the concentration-response curves may be flattened at high concentrations of isoproterenol. This is likely to be the case when the isoproterenol response (largely generated by the transfected AC9 variant) is higher than the standardizing stimulus that is largely produced by the host cell adenylyl cyclases. Therefore, in this study we only report results where the isoproterenol-induced response was less than 80% of the standardization stimulus. Expression of HAFLAG-tagged AC9 proteins was examined by SDS-PAGE and immunoblotting of

extracts prepared from crude membranes of transfected HEK293 FT cells as reported previously [10,13]. Protein blots were reacted with the 12CA5 Anti-HA (Abcam, Cambridge, UK)) or M2 anti-Flag mouse monoclonal antibodies (Sigma-Aldrich, Poole, Dorset UK), using secondary anti-mouse IRDye® 680RD-tagged goat anti-mouse IgG from LiCor with fluorescence read-out in a LiCor Odyssey imager.